



Contents lists available at ScienceDirect



## Review

## Physical properties of cytoplasmic intermediate filaments☆

Johanna Block <sup>a</sup>, Viktor Schroeder <sup>a,b</sup>, Paul Pawelzyk <sup>c</sup>, Norbert Willenbacher <sup>c</sup>, Sarah Köster <sup>a,b,\*</sup><sup>a</sup> Institut für Röntgenphysik, Georg-August-Universität Göttingen, Göttingen, Germany<sup>b</sup> Center for Nanoscale Microscopy and Molecular Physiology of the Brain, Göttingen, Germany<sup>c</sup> Institute of Mechanical Process Engineering and Mechanics, Karlsruhe Institute of Technology (KIT), Karlsruhe, Germany

## ARTICLE INFO

## Article history:

Received 13 March 2015

Received in revised form 28 April 2015

Accepted 5 May 2015

Available online xxxx

## Keywords:

Intermediate filament

Cell mechanics

Assembly

Persistence length

Polyelectrolyte

Network

## ABSTRACT

Intermediate filaments (IFs) constitute a sophisticated filament system in the cytoplasm of eukaryotes. They form bundles and networks with adapted viscoelastic properties and are strongly interconnected with the other filament types, microfilaments and microtubules. IFs are cell type specific and apart from biochemical functions, they act as mechanical entities to provide stability and resilience to cells and tissues. We review the physical properties of these abundant structural proteins including both *in vitro* studies and cell experiments. IFs are hierarchical structures and their physical properties seem to a large part be encoded in the very specific architecture of the biopolymers. Thus, we begin our review by presenting the assembly mechanism, followed by the mechanical properties of individual filaments, network and structure formation due to electrostatic interactions, and eventually the mechanics of *in vitro* and cellular networks. This article is part of a Special Issue entitled: Mechanobiology.

© 2015 Elsevier B.V. All rights reserved.

## 1. Introduction

Eukaryotic cells need mechanical properties, which are adapted to their specific function, in order to perform in the context of tissues and organisms. It has been recognized for some time that the cytoskeleton, a composite network of filamentous proteins, along with corresponding linker proteins and molecular motors is a highly mobile, viscoelastic and flexible entity, which determines cell mechanics to a great extent [1]. Actin-based microfilaments (MFs) and tubulin-based microtubules (MTs) are polar filaments and both interact directly with the molecular motors myosin or kinesin and dynein, respectively. Furthermore, numerous MF or MT binding proteins with varying length, stiffness and binding sites are known. By contrast, intermediate filaments (IFs) are non-polar objects, which implies that they do not act as tracks for translational molecular motors. However, IFs do interact with molecular motors as cargo [2,3] and could even serve as a means to "store" molecular motors in cells.

Each type of cytoskeletal filament has a specific role in the cell. To name a few examples, as an exhaustive list would go beyond the scope of this article, MFs form stress fibers for cell contraction, the cortex underneath the cell membrane and protrusions like lamellipodia, filopodia and pseudopodia; MTs enable transport of cargo through the cell and act as compression-bearing mechanical elements; the role of IFs is less well

studied from a biophysical point of view but it is widely accepted that these structural proteins contribute considerably to cell mechanics. An interesting aspect that has been stressed recently is the contribution of different IF proteins to the varying and adapted mechanical properties of different cell types. IFs are the only cellular protein fibers that are, besides the cytoskeleton, also found in the nuclear lamina. Contrary to cytoskeletal IFs, nuclear lamins are universal in metazoans. In this review we will, however, focus on cytoskeletal IFs.

IFs are linked to each other, to the other cytoskeletal components and to other cellular structures, such as desmosomes and hemidesmosomes or intercalated disks by intermediate filament associated proteins (IFAPs). Thus, IFAPs are an important ingredient of IF mechanics in cells. A comprehensive overview of these building blocks can be found in Ref. [4]. Probably the most well-known IFAP is plectin, a member of the plakin family, which binds all types of IFs, MFs and MTs, as well as a number of other cellular structures [1,5].

Due to a number of recent evidences that IFs specifically play an important role in cell mechanics and that this role is closely linked to disease, it is very timely to summarize the physical properties of IFs, their networks, bundles and structures in living cells. In order to maintain a consistent terminology, we will refer to the development of extended filaments from subunits (e.g., tetramers) as filament assembly and to the development of entangled or cross-linked networks from these extended filaments as network formation.

We have structured our review in a bottom-up approach and begin by explaining the standard assembly mechanism as well as alternative pathways specific to IFs in Section 2. Thereby we lay a basis for the understanding of the mechanical properties of IFs, many of which are

☆ This article is part of a Special Issue entitled: Mechanobiology.

\* Corresponding author at: Institut für Röntgenphysik, Georg-August-Universität Göttingen, Göttingen, Germany. Tel.: +49 551 399429; fax: +49 551 399430.

E-mail address: [sarah.koester@phys.uni-goettingen.de](mailto:sarah.koester@phys.uni-goettingen.de) (S. Köster).

encoded in their particular architecture. Another specialty of IFs with respect to MTs and MFs is the cell type and organism specificity of the exact amino acid sequence and we continue in **Section 3** by shedding light on the role of this specificity in health and disease. **Sections 4 and 5** are concerned with the mechanical and polyelectrolytic properties, respectively, of readily assembled, individual filaments. These filaments are the building blocks of intricate networks found in the cell or formed *in vitro* and thus a thorough understanding of their physical properties is instrumental for understanding the emerging properties of higher-order structures like bundles and networks. **Section 6** is dedicated to the mechanical properties of *in vitro* assembled entangled or cross-linked networks of IFs and **Section 7** presents the few existing studies on IF mechanics in cellular systems. **Section 8**, finally, summarizes the review and aims to anticipate future research directions.

## 2. Intermediate filament architecture

### 2.1. Assembly mechanisms

All IF proteins share a secondary structure consisting of an  $\alpha$ -helical 'rod' domain that is flanked by unstructured 'head'- and 'tail'-domains at the N- and C-terminus, respectively. The central rod domain contains three coil domains which are separated by linker domains. In contrast to MTs and MFs, IFs assemble in a hierarchical manner. Two elongated protein subunits form a parallel coiled-coil homo- or heterodimer, depending on the particular protein, and assemble further to an anti-parallel so-called A11-tetramer. Because of this anti-parallel symmetry of the tetramer, the assembled tetramers are not polar. Tetramers then associate laterally to form unit-length filaments (ULFs) of about 65 nm length [6]. Elongated,  $\mu$ m-long filaments emerge by longitudinal annealing of ULFs [7] (Fig. 1A), consequently the mature filaments are also non-polar. For some IF proteins, the fully assembled filaments show a lateral compaction step after the filament formation (see Table 1) [8].

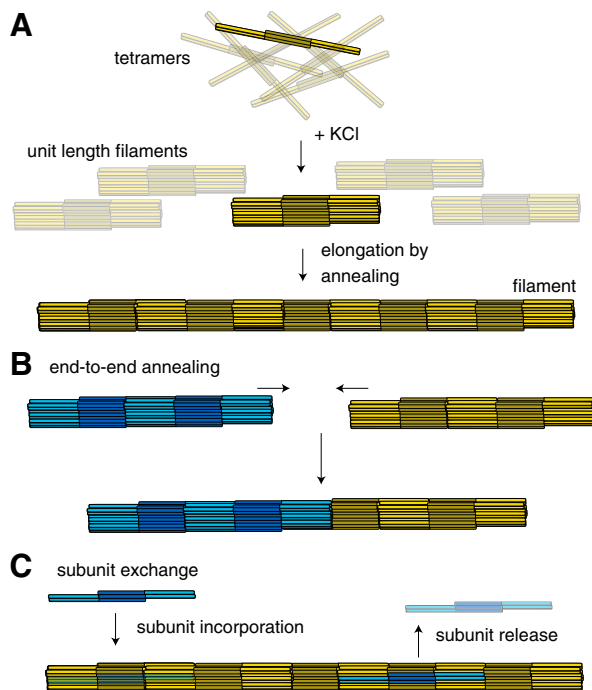


**Fig. 1.** Assembly of intermediate filaments including alternative pathways (on the example of vimentin; without the compaction step). (A) Tetramers anneal laterally to form unit-length filaments (ULFs). Full-length filaments are formed by longitudinal assembly. (B) Elongated filaments are also formed by end-to-end annealing. (C) Individual subunits are incorporated in and released from fully assembled, mature filaments.

The hierarchical assembly mechanism differs significantly from the one exhibited by the other types of cytoskeletal filaments, MFs and MTs, where globular proteins polymerize in a polar way and the assembly mechanism involves nucleoside triphosphates. Interestingly, the assembly pathway of IFs, and in particular the fact that several subunits per cross-section are involved, encodes many of the physical properties of these filaments, as described below.

*In vitro*, IF proteins can be solubilized by chaotropic agents like 8 M urea. The assembly of intermediate filaments is then initiated by adding salt at physiological concentrations (e.g., in the case of vimentin) or decreasing the pH from 9 to about 7 (e.g., in the case of keratin). The principle assembly mechanisms for several IF proteins were elucidated mainly by employing electron microscopy (EM) [6,8] and atomic force microscopy (AFM) [7,10]. More recently, small-angle X-ray scattering (SAXS) has been used as well to obtain structural data of the assembly steps [11,12]. In combination with microfluidic methods, SAXS has been adapted to study the different assembly states for vimentin up to the ULF level *in situ* thus determining that the ULF formation takes place on a time scale of a second [13].

For several IFs, including keratins, vimentin, desmin, and neurofilaments, it has been shown that their cross-sectional diameter is not uniform along their length [6,8,14,15]. Instead, filaments typically have a varying number of tetramers per cross-section, which corresponds to a varying mass-per-length (MPL) [14,15]. For vimentin, this polymorphism is larger when the assembly *in vitro* is initiated in a "kick-start" mode, by fast addition of the salt-containing assembly buffer – as compared to slower methods, such as dialysis into the assembly buffer [6,8]. This polymorphism ranges from 4 to 13 tetramers under physiological conditions, while the standard configuration contains eight tetramers [6,8].

Assembly speeds differ considerably between IF proteins, e.g., keratins assemble into extended filaments within seconds, whereas vimentin, desmin and neurofilaments at this time point only form ULFs [8]. For vimentin, it was found that the time to reach a certain mean filament length is inversely proportional to the concentration and the filaments assemble at a speed of 0.2 nm/( $\mu$ M·s) [10]. For keratin such a systematic concentration dependence was not investigated so far, but individual values hint at a speed of about 23 nm/( $\mu$ M·s) [9]. For comparison, MFs and MTs assemble at speeds of few nm/( $\mu$ M·s) [16,17]. Furthermore, the assembly depends on the temperature [8] and on the ions present. This latter aspect is discussed in detail below.

### 2.2. Alternative assembly mechanisms

In contrast to MFs and MTs, the specific architecture of IFs and in particular the high number of subunits per cross section and the fact that nucleoside triphosphates are not involved in the assembly, give rise to alternative principle assembly pathways. The most straight forward one of such mechanisms is end-to-end annealing of filaments, where two assembled filaments attach and form a longer filament (Fig. 1B). This phenomenon was observed in cell experiments for vimentin and neurofilaments [18,19] as well as *in vitro* for purified vimentin [20,21]. For the cell experiments, two cell types with differently labeled vimentin filaments were fused. After incubation, filaments with contiguous segments of alternating colors were observed, which indicates end-to-end annealing [18]. For the *in vitro* experiment, the authors

**Table 1**

Assembly details for different IF proteins at "standard" assembly conditions; data from Ref. [8,9].

IF protein	Type	Monomers/cross-section	Compaction step
Keratin (K8/K18)	I, II	16–21	No
Desmin	III	47	Yes
Vimentin	III	30–44	Yes
Neurofilaments (NF-L)	IV	19–43	

mixed differently labeled, assembled vimentin populations to directly observe the end-to-end annealing of filaments by total internal reflection microscopy (TIRFM) [20] and confocal microscopy [21].

Additionally, exchange of individual subunits along the assembled filament (Fig. 1C) was observed, again in cells [18,22–24] and *in vitro* [21]. In living cells, soluble vimentin subunits [25] were incorporated into existing filaments [22–24]. This was first observed for chicken vimentin expressed in mouse fibroblasts, using immunofluorescence and immunoelectron microscopy [23,24]. Here, newly expressed vimentin was detected to be incorporated into the existing filament network at various sites. Furthermore, fluorescence recovery after photo bleaching (FRAP) was used to investigate the exchange of microinjected labeled vimentin complexes with full filaments in fibroblasts [26]. It could be shown that bleached vimentin fibers recover their fluorescence without any distinctive polarity. Photobleaching and photoactivation methods as well as cell fusion were employed to show ‘intercalary subunit exchange’ for vimentin and neurofilaments [18]. This process occurs evenly along filaments, without a preference for the filament ends.

*In vitro*, the incorporation and release of labeled vimentin subunits was quantitatively measured. It could be shown that the exchange of subunits depends on the cross-sectional polymorphism of the filaments. Filaments with a heterogeneous mass-per-length show a faster exchange of subunits than more uniform filaments. It is hypothesized that “looser” binding of subunits in highly polymorphic filaments causes this more pronounced exchange. Also, polymorphic filaments might have more binding sites, “loose ends”, to incorporate subunits from solution. Subunit exchange occurs on slower time scales than the hierarchical assembly described above. While ULFs are formed from tetrameric vimentin within seconds [13] and filaments assemble from ULFs within minutes [7], less than 1% of the subunits in a filament are exchanged per hour [21]. Polymorphism and subunit exchange might play a role in the stability of IF networks in cells. Since the polymorphism might lead to differing mechanical properties of the filaments, local gradients of the soluble subunit concentration could enable cells to alter the filament network. The fact that the results from *in vivo* and *in vitro* experiments are comparable, suggests that subunit exchange is an intrinsic property of IFs and does not require cellular factors.

Another aspect governing the state of intermediate filaments is the phosphorylation of the head domain, which leads to disassembly of filaments and networks [27,28]. This mechanism allows cells to maintain the equilibrium between filaments and a soluble pool of tetrameric IF protein.

### 3. Types of intermediate filaments

Apart from their architecture, probably the most striking difference between IFs on the one hand and MFs and MTs on the other hand, is the organism- and tissue-specificity of IFs (see Fig. 2). The term “intermediate filament proteins” is used to describe a large class of proteins encoded in around 70 genes in human [29]. IFs are classified into five types (see also Tables 1 and 2; type V IF, lamins, are not listed as this is beyond the scope of this review) according to domain and sequence homology [30]. Whereas the proteins all share a common secondary structure, differences in the amino acid sequence lead to striking differences in assembly pathway, dynamics and speed, persistence length, charge- and hydrophobicity patterns, aggregation behavior and structure formation *in vitro* and in the cell. Some of these aspects are discussed in the present review. Thus, by the “choice” of IF type (or combination of different types), cells have a handle to tune their physical appearance including the mechanical properties. The reversible epithelial-mesenchymal-transition (EMT) is a famous example where such adaptation takes place even temporarily and keratin-rich epithelial cells are transformed into vimentin-rich mesenchymal cells. From a functional perspective, epithelial cells form cell-cell contacts while mesenchymal cells lose these contacts and gain migratory properties. Due to the

varying mechanical properties of IFs on the single filament level as well as for networks thereof *in vitro* and in the cell, it has been suggested by the community that IFs are a “mechanical footprint” of a specific cell type.

Evolutionary, all IFs stem from an *ur-lamin*, which was found even in primordial organisms such as *Hydra attenuata*. In general, higher animals accommodate a larger variety of different IFs; e.g., *Drosophila melanogaster* expresses lamins A and B, but no cytoskeletal IFs and *Caenorhabditis elegans* expresses the lamins and eleven cytoplasmic IFs [32]. Even though most work on IFs has been performed on mammalian cells, IF or IF-like cytoplasmic proteins are also found in insects [32].

As diverse as the IFs themselves are the associated diseases. In Ref. [31], the authors state that more than 80 diseases are caused by mutations in IFs. Examples are skin disorders, amyotrophic lateral sclerosis (ALS), Alexander disease and progeria (premature aging).

### 4. Mechanical properties of single IFs

As described in Section 2, IF proteins form extended filaments that can reach lengths of several micrometers. The mechanical stiffness of such biopolymers or -filaments can well be quantified and characterized by the so-called persistence length  $L_p$ , which describes the distance along which the filament direction does not considerably change and can be written as the bending rigidity  $\kappa$  in units of  $k_B T$ :  $L_p = \kappa/(k_B T)$ . The biopolymer network properties depend on the characteristics of the individual filaments and, thus, much effort has been devoted to the determination of the persistence length of individual IFs of different types.

#### 4.1. The persistence length $L_p$ of IFs

When compared to MFs and MTs, the persistence length of IFs is rather short, meaning that IFs are more flexible: Whereas the persistence length of MFs lies in the range of 7 to 22 μm and MTs even reach several mm (see, e.g., Ref. [33]), the persistence lengths of IFs were consistently determined to lie in the range of a few hundred nm and a few μm. Thus, from a physical point of view, IFs are classified as semi-flexible biopolymers and are about one order of magnitude more flexible than MFs [34,35].

However, the numeric values for different types of IFs vary considerably. In particular, neurofilaments are much softer than the other studied cytoskeletal IFs keratin, vimentin and desmin. Additionally, the results from different experimental protocols and techniques for measurements on the same type of IFs deviate to a certain degree, as can be seen in Table 2 where we summarize the existing measurements of the persistence length of IFs. As it is very difficult to infer persistence lengths of polymers larger than  $L_p \sim 100$  nm, the deviation can most likely be attributed to different techniques used.

The earliest determination of the persistence length of an IF was performed on desmin [38] by quasi-elastic light scattering. From measurements on desmin networks and modeling semi-flexible polymers, the authors derived a lower and an upper limit of 0.1 μm and 1 μm, respectively. The dynamic shear modulus of filament networks at high frequencies is dominated by the relaxation of single filament segments [44]. This correlation has been used to deduce the persistence length from corresponding rheological data and for desmin a value of  $L_p = 0.9$  μm was found [39].

For vimentin, rheology measurements yield a value of merely 0.4 μm [39]. However, when adsorbed on various solid supports and analyzed by AFM or EM, a numerical value of 1 μm was found [40]. Under vitrified conditions and without any chemical fixation, using cryo-electron microscopy, vimentin IFs were found to contain compact elements with a persistence length of several μm, interrupted by flexible regions, where the filaments are unraveled and softer [45]. Thus, for most studies of the persistence length of IFs the filaments were either incorporated in a network and probed by rheological methods (see also Section 6)

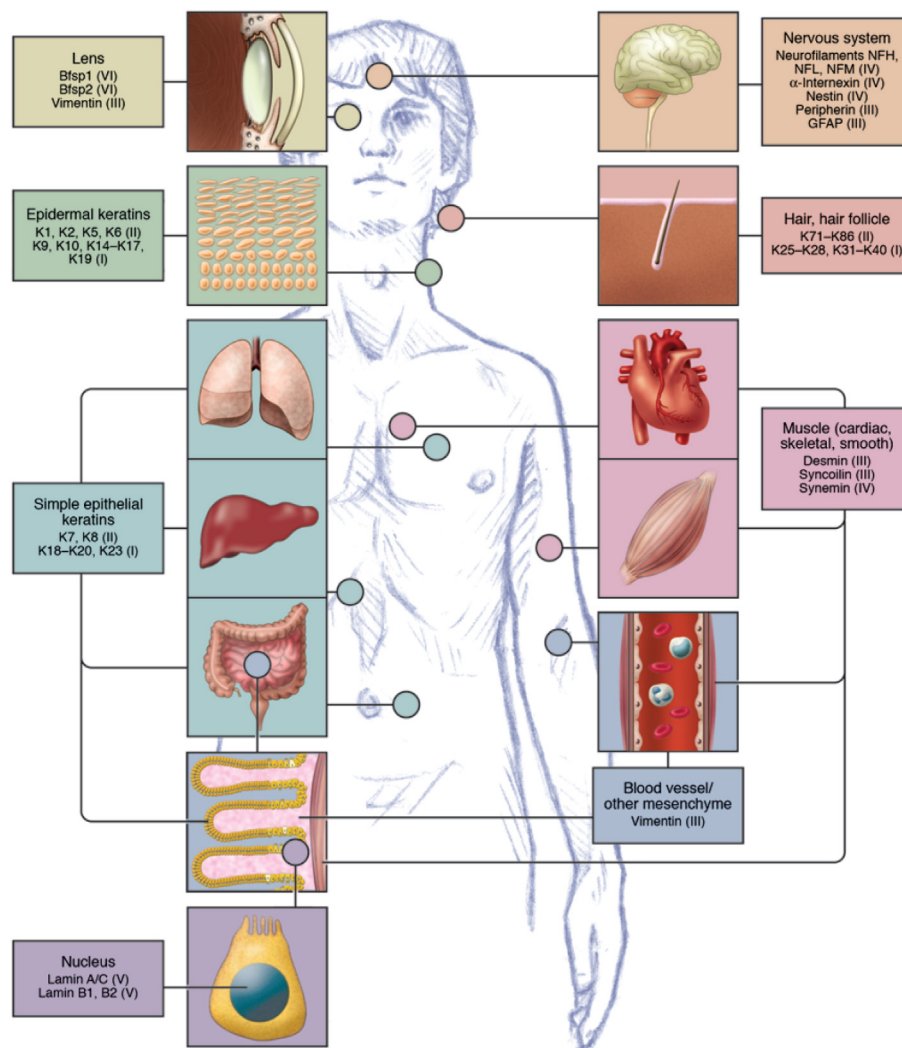


**Fig. 2.** Tissue specificity of different types (I–V, in parentheses) of IFs. Nuclear lamins are conserved in all metazoan cells, whereas cytoskeletal IFs vary between cell types and are hypothesized to determine the specific mechanical properties of the cells and thereby the (biophysical) function; reproduced from Ref. [31].

or adsorbed on a substrate and imaged with high resolution EM or AFM. To avoid this influence of either other filaments or a substrate, we measured the persistence length of freely fluctuating vimentin IFs confined in a narrow channel and of freely fluctuating vimentin IFs restricted to the focal plane by glass plates. The resulting values are  $L_p = 2.1 \pm 0.1 \mu\text{m}$  and  $L_p = 2.0 \pm 0.5 \mu\text{m}$ , respectively [34].

Keratin, as well, has been studied by rheology ( $L_p = 0.65 \mu\text{m}$ ) [37] and EM ( $L_p = 0.3\text{--}0.48 \mu\text{m}$ ) [9]. Additionally, results from stiffness measurements by direct mechanical stretching of a keratin-like protein

from hagfish slime threads provide a persistence length of  $0.85 \mu\text{m}$ , which is very consistent with these findings [36]. As this protein has a lot in common with IFs such as similar sequence and assembly pathway and is secreted as a mostly pure, near-perfectly aligned bundle, it was used as a model system for hydrated IFs in these studies. This method involves the measurement of the Young's modulus  $E$  and calculation of the persistence length from the second moment of inertia  $I$  via  $\kappa = EI$ . Thus, the radius of the filament enters as a power of 4 and given the heterogeneity in diameter, the approach might not be straightforward for IFs.

Furthermore, neurofilaments have been characterized regarding their persistence length. Here,  $L_p$  depends on the subunit protein ratio of NF-L, NF-M and NF-H and the monovalent salt concentration, which influences the effect of entropic repulsion versus electrostatic ionic bridging of the (long) side arms in neurofilaments. Values between 0.05 and  $0.2 \mu\text{m}$  were found [42].

An effect of buffer ion concentration on the persistence length was investigated by Lichtenstern et al. They found by EM that when assembled in the absence or presence of  $1 \text{ mM MgCl}_2$ , keratin K8/K18 has a persistence length of 0.3 or  $0.48 \mu\text{m}$ , respectively [9]. The influence of ions on assembly and bundle or network formation is described in more detail in Section 5. The measured persistence length of freely fluctuating vimentin filaments [21] and the one of filaments that are adsorbed to a surface [40] is different suggesting an influence of the

**Table 2**  
Persistence lengths of different IF biopolymers.

IF protein	Type	$L_p [\mu\text{m}]$	Experimental technique	References
Keratin-like	(I, II)	0.85	Direct mechanical stretching	[36]
Keratin (K8/K18)	I, II	0.65	Rheology	[37]
		0.3–0.48	EM	[9]
Desmin	III	0.1–1	Quasi-elastic light scattering	[38]
		0.9	Rheology	[39]
Vimentin	III	1	AFM, EM	[40]
		0.4	Rheology	[39]
		2–2.1	Fluorescence microscopy	[34]
		0.5	Bulk rheology	[41]
Neurofilaments	IV	0.05–0.2	AFM	[42]
		0.2	Not known	[44]
		0.2	Bulk rheology	[41]

underlying substrate. One possible explanation is that the filaments bend more strongly during the adsorption process. Neurofilaments are a lot softer than the other studied intermediate filaments. This finding fits to the properties of the cell types where the filaments are mainly expressed in, as neurons are also much softer than muscle cells, connective tissue or epithelial cells. IFs in the cellular context are discussed in Section 7.

#### 4.2. Single molecule mechanics of IFs

Apart from the bending rigidity or persistence length, a polymer is mechanically characterized by its stretchability. To date, there are only few direct measurements on individual filaments available, probably at least partly due to the experimental challenges involved. In most of the publications on this topic that are reviewed here, the lateral displacement of IFs adsorbed to solid supports was analyzed by AFM [46,47]. As a further development, Guzman et al. used a nanostructured substrate with 250 nm diameter holes to reduce the influence of the underlying substrate on the IFs during their AFM experiments. They measured individual vimentin IFs that were spanned over such a hole [48]. Furthermore, Ramm et al. made use of an optical tweezers setup combined with Brownian dynamics simulations to gain insights into the folding and stability of the coil 2B of vimentin IFs [49]. To the best of our knowledge there are no other single molecule experiments for intermediate filaments so far.

From network measurements there is evidence for an enormous elongation potential in IFs (reviewed in detail in Section 6). Lateral bending measurements performed by Kreplak et al. for individual recombinant murine desmin IFs, recombinant human keratin K5/K14 IFs and neurofilaments from rat brain directly confirmed this hypothesis. The average extensibility of these three IFs on a mica surface is 2.8-fold, 2.3-fold and 2.6-fold, respectively [46]. Moreover, for desmin IFs they found a maximum stretch of 3.6-fold the initial length of a filament, which was accompanied by a significant reduction in the filament diameter [46]. This result was confirmed three years later by the same group, where they stretched recombinant human and murine desmin IFs up to 3.4-fold the initial length with a maximum force of about 3.5 nN [47].

Such extreme extensions most probably originate from the specific architecture of IFs and are consequently not found in MFs or MTs, which are build up from globular monomers and contain only one or very few monomers per cross-section. During elongation of the filaments, molecular adaptions are necessary. One possibility is the  $\alpha$ -helix-to- $\beta$ -sheet transition ( $\alpha \leftrightarrow \beta$  transition) of the coiled-coil domain of each dimer [36,46]. This transition was first described for wool using X-ray diffraction to distinguish the two states [50]. The observation is consistent with a decreased filament width [51] but accounts only for about a factor of two in length [46,52]. Therefore, further alterations in the molecular structure of the filaments are necessary to explain the observed extension. One explanation could be a stretching/unfolding of the flexible N- and C-terminal domains of the monomers [36,46]. Additionally, there is evidence for axial sliding of the subunits of the filament relative to one another [40,48]. The idea is that sections of individual tetramers or protofibrils detach and “lock in” a few units further down. This mechanism would also lead to a thinning of the filaments as seen, e.g., in Fig. 7 of Ref. [47].

Another interesting finding in this context is the force- or extension-dependent reaction of IFs. For small extension (less than 10 to 100% [47,48]) or at low forces (60 to 130 pN [47]), the filaments seem to act fully elastic. At higher forces and further extension a plastic behavior/deformation accompanied by strain hardening and a decrease in diameter is observed [46–48]. As a tensile strength for desmin a value of 240 MPa was found [47]. For vimentin, a bending modulus in the range of 300 to 900 MPa was found, where the value is at the higher end for glutaraldehyde fixed filaments [48]. All these experiments provide important insights into the mechanical properties of IFs. What

is still largely missing, however, are measurements of non-adsorbed individual IFs, freely fluctuating in physiological buffer and therefore without any interactions with a substrate.

As mentioned above, Ramm et al. did not analyze whole filaments but the coil 2B part of vimentin dimers. In their study, two modified coil 2B molecules were used – one was cross-linked at the N-terminus and equipped with a DNA-ubiquitin handle for optical trapping at the C-terminus, while the other one was modified the other way around. From these experiments they found that unzipping the coiled coil requires different forces depending on the respective starting point. The molecule was highly resistant against pulling/unzipping from the C-terminus compared to pulling/unzipping from the N-terminus. Analyzing energy profiles they defined three regions of stability in coil 2B, a labile N-terminal end, a medium stable middle section and a highly stable C-terminus. According to the authors the stability of the C-terminal end of coil 2B could be important for assembly, ensuring that the coiled coil stays zipped and stabilizes the IFs on the dimer level [49].

#### 4.3. Simulations of IF mechanics

In addition to experiments as reviewed above, simulations provide an alternative and complementary way to understand biopolymer mechanics. To date, only few simulations of the mechanical behavior of parts of IFs exist and the field is only recently evolving. With different levels of accuracy, ranging from atomistic to coarse-grained representations, Qin et al. simulated dimers and tetramers of vimentin aiming a better knowledge of the great extensibility, stiffness and mechanical resistance of IFs [52–54], as shown in Fig. 3. Comparing their results from *in silico* studies with results from *in vitro* experiments [47,48] they demonstrate a good agreement for their structural estimates as well as for the mechanical properties of the IFs [52]. Ramm et al. performed simulations to further validate their experimental results and verify the deconvolution performance. By mimicking their experiment they obtain good agreement of results received from experiment and simulation [49].

#### 5. Polyelectrolyte properties of IFs

Depending on the amino acid sequence and the pH of the solution, the charge of IF proteins can be estimated (for a representation of such charge patterns on IFs compared to other biological filaments, see Fig. 4A). At pH 7.5, vimentin monomers carry a charge of  $-19\text{ e}$  leading to a line charge of  $-14\text{ e/nm}$  or a surface charge of  $-0.07\text{ C/m}^2$  for a 10-nm-diameter filament with 32 monomers per cross-section [55]. By contrast, keratin K8 and K18 carry  $-6\text{ e}$  and  $-11\text{ e}$  per monomer, respectively, leading to a line charge of  $-3\text{ e/nm}$  or a surface charge of  $-0.02\text{ C/m}^2$  for a 10-nm-diameter filament with 16 monomers per cross-section. The line charge of desmin lies in-between, at  $-6\text{ e/nm}$ . These estimates show already very clearly, that despite the structural similarities between IF proteins, the differences in the amino acid sequence lead to varying charge and hydrophobicity patterns. Thus, to fully describe IFs not only their polymeric nature, but also their polyelectrolytic properties have to be taken into account.

The examples above show that IFs, like many other intracellular biological filaments, are negatively charged and therefore interact strongly with cations (see Fig. 4B). Interestingly, extracellular filaments are usually less highly negatively charged [56]. When discussing the interaction of IFs with ions, we have to distinguish two cases. When unassembled tetramers are mixed with ion-containing buffers, the ions influence the assembly process. By contrast, if the filaments are first fully assembled (e.g., by addition of at least 50 mM monovalent ions like  $\text{K}^+$  or  $\text{Na}^+$  to vimentin) and then exposed to other ion species, the interactions are mostly between the filaments and the counterions.

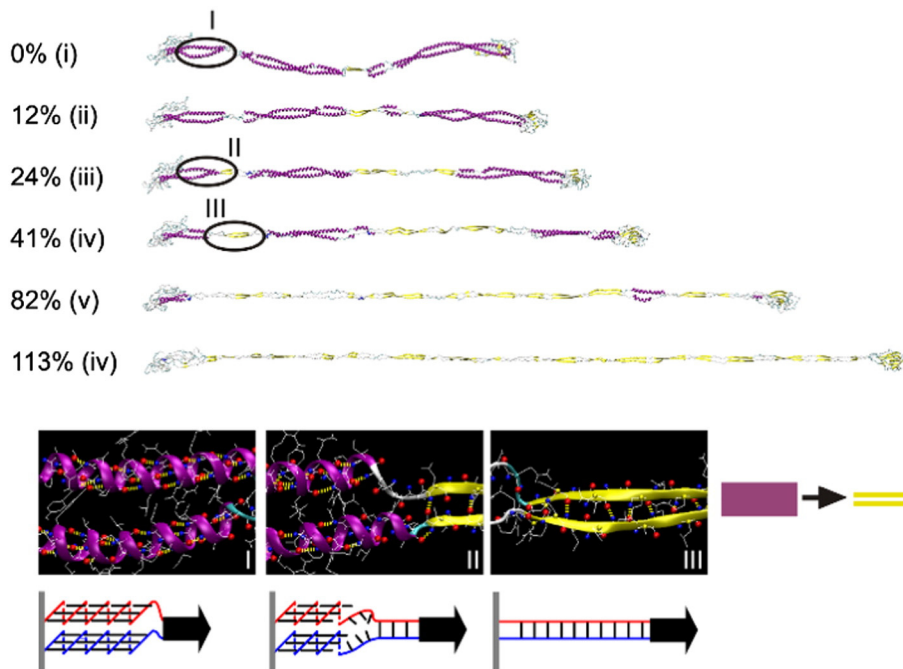


**Fig. 3.** Possible mechanism involved in extensibility of IFs. Simulation snapshots and structural analysis during pulling of an IF dimer. Upper part shows dependence on applied tensile strain; lower part depicts snapshots of the right part of coil 1A as highlighted above. Atomistic details of the  $\alpha \leftrightarrow \beta$  transition are sketched below the snapshots; reproduced from [51].

### 5.1. Influence of ions on assembly

Whereas the influence of monovalent ions on IFs assembly has been extensively studied and the sub-steps involved in the assembly are well characterized (see Section 2) [6,59], the effect of the addition of di- or multivalent ions is less well understood. Early on, it was found for desmin filaments that they grow thicker in the presence of  $\text{Ca}^{2+}$  than in the presence of  $\text{Na}^+$ . The differences cannot merely be explained from differences in ionic strength  $I = \frac{1}{2} \sum_i c_i z_i^2$ , which takes into account the concentration  $c_i$  and valence  $z_i$  of the different ion species  $i$ . Further principle differences in valences must also play role [60]. In addition to valence, other ion-specific properties like size play role as could be observed in the difference of vimentin assembled in the presence of  $\text{Mg}^{2+}$  or with  $\text{Ca}^{2+}$  [61]. Interestingly, the differences are found mostly in the diameter of the filaments rather than in the build-up along the filament (axial repeat). Clearly, concentration also plays a role and higher concentrations of  $\text{Mg}^{2+}$  lead to thicker vimentin filaments which also appear as less well organized [8,12,62,63]. Thus, the influence of different ion species, valences and concentration is complex and open questions remain.

When adding several different ion species simultaneously during assembly, competitive effects can be observed. Thus, there are strong indications that  $\text{Mg}^{2+}$  hinders and thereby slows down vimentin assembly. Excess monovalent ions outperform this effect and in that case  $\text{Mg}^{2+}$  affects rather the filament surface or substructure in a coordinated way [12]. This is in agreement with the observation that in the presence of monovalent ions, both  $\text{Mg}^{2+}$  and  $\text{Ca}^{2+}$  ions induce identical cross-linking of the networks as indicated by rheology studies [64,41,65].

Keratin assembly can *in vitro* be initiated by decreasing the pH of the solution from 9 to 7 or 7.5 and additional ions in the assembly buffer lead to interesting structure formation. Thus, keratin K8/K18 IFs form networks of bundles in buffers containing 100 mM KCl and 1 mM  $\text{MgCl}_2$ , which are added simultaneously [57,66], as well as in the presence of merely  $\text{MgCl}_2$  above a concentration of 1 mM [67]. Consequences on rheology measurements [68] are discussed in further detail below. Fig. 4C shows how sensitive the kinetics of keratin assembly and bundle formation depend on protein concentration  $c_k$ , temperature and addition of salt.

Neurofilaments are particularly interesting when it comes to charge interactions due to their particular architecture with extended side arms whose polyampholytic nature allows for matching of positive and negative charges, called “hand shake” by the authors of Ref. [42].

### 5.2. Influence of ions on aggregation and network formation

In the previous paragraph we have reviewed studies, where one or several species of ions are added simultaneously *during assembly*. In bulk experiments this is usually the only experimental possibility since it is not easily possible to mix ions into a fully assembled, entangled network. Novel microfluidic approaches, however, rely on small sample volumes and thus diffusive mixing times are small due to the relation between time and length scales  $t = \frac{x^2}{2D}$ , with the diffusion coefficient  $D$ . Thus, in continuous flow microfluidics [13] or droplet microfluidics [58,69] multivalent ions have been added to already partially or fully assembled filaments. These methods furthermore offer the possibility to adjust the experimental time scales exactly to the studied systems and processes.

In general, when bringing a charged filament into a buffer containing mono-, di- and/or multivalent ions screening effects lead to a decay of the potential at the charged filament surface in the electrolyte solution, which can be understood from the competition between electrostatic energy gain by condensation of counterions to the charged interfaces and entropy gain by Brownian motion of the ions.

“Titration” of vimentin filaments with different concentrations of  $\text{Mg}^{2+}$  shows that above a threshold concentration of 10 mM the filaments strongly aggregate on a minute time scale as shown in Fig. 4D [58,69]. On a filament level, the aggregation process manifests itself in a “zipping together” of the IFs (see Fig. 4E for an example). For trivalent  $\text{Co}(\text{NH}_3)_6^{3+}$  ions the threshold is about one order of magnitude lower at  $\sim 1$  mM [55,69]. This threshold can be explained by considering competitive binding of the mono- and the multivalent ions on the surface of the filaments. In the case of vimentin, about 50% of the ions on the surface have to be multivalent in order to mediate aggregation [55].

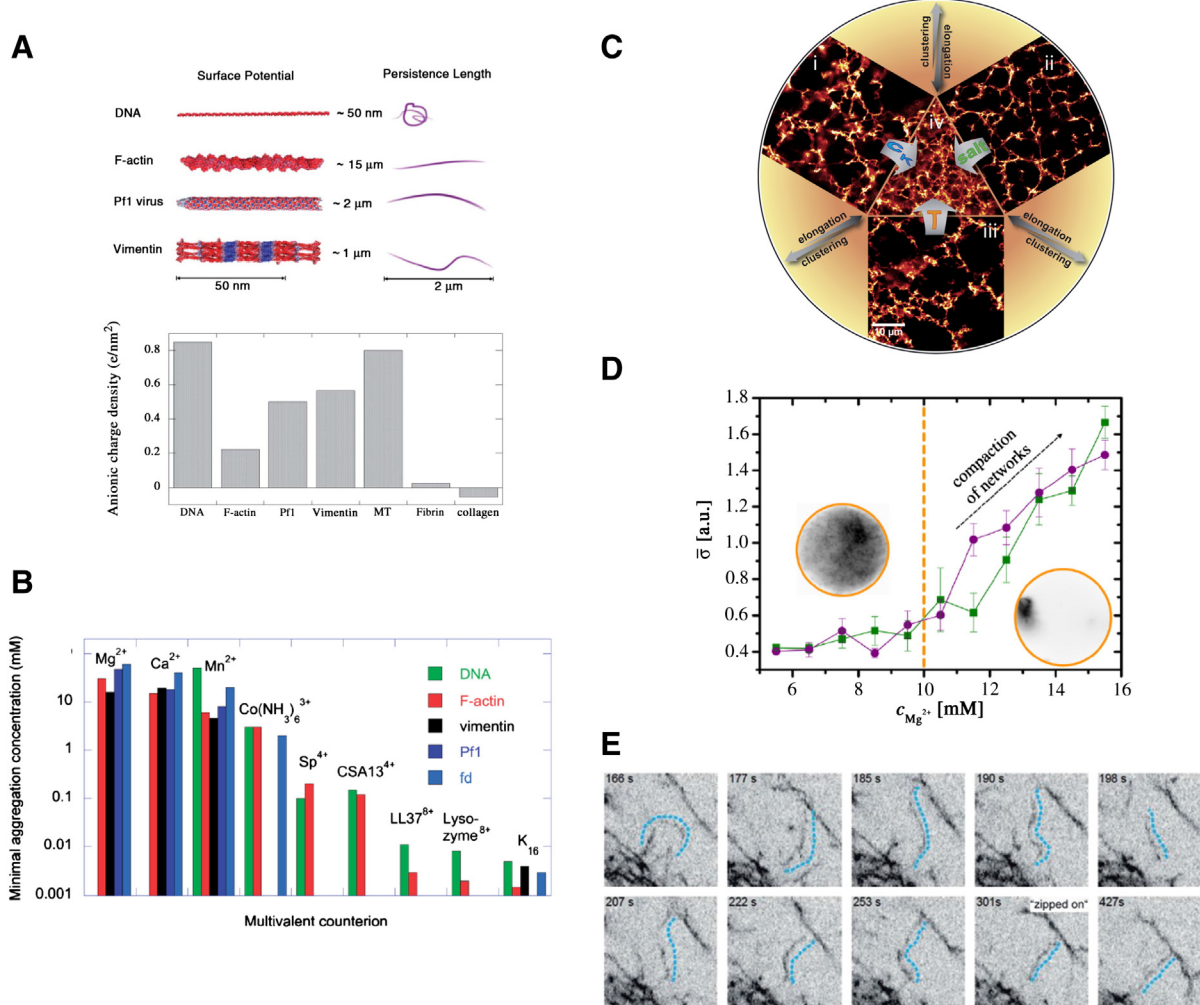


**Fig. 4.** Polyelectrolyte properties of IFs. (A) Vimentin carries a distinct charge pattern which differs from other biological polyelectrolytes and from other IFs and leads to a vimentin typical aggregation behavior; reproduced from Ref. [55]. (B) Minimal aggregation concentrations for different biological polyelectrolytes including vimentin IFs and different ion valences; reproduced from Ref. [55]. (C) Keratin bundling depends on protein concentration, salt and temperature; reproduced from Ref. [56]. (D) The threshold for vimentin with  $\text{Mg}^{2+}$  is directly observable (fluorescence, inverted gray scale) in an aggregation experiment employing microfluidic picoliter drops; reprinted with permission from Ref. [57] Copyright 2012, AIP Publishing LLC. (E) Fluorescence imaging (inverted gray scale) shows the “zipping together” of individual filaments during aggregation; reproduced from Ref. [54].

In addition to the IF protein specific charge pattern, the differing amino acid sequences also lead to specific hydrophobicity patterns which contribute to the degree and nature of inter-filament interactions. Thus, e.g., in keratin, hydrophobic amino acid clusters located in the central rod domain lead to string attraction of the filaments at these contact points [37].

## 6. Mechanical properties of reconstituted IF networks

As reviewed above, IF proteins form semi-flexible, charged polymers and it is certainly important to characterize these individual filaments as a basis for understanding cell mechanics. However, when networks are formed from the filaments, new properties emerge and the study of these properties has constantly attracted researchers over the years. Interestingly, semi-flexible IFs form predominantly elastic networks when a critical concentration is exceeded, which is more than three magnitudes lower than for synthetic polymers [70]. This critical concentration is typically below 0.5 g/l [39,71,72], e.g., K8/K18 forms viscoelastic networks at concentrations as low as 0.1 g/l [68,73]. Such networks exhibit interesting viscoelastic response when exposed to external stress or strain fields.

The kinetics of the network formation have been characterized by the temporal evolution of the elastic storage modulus  $G'$  and the viscous

loss modulus  $G''$  as obtained from oscillatory shear experiments at a constant frequency. Such experiments are performed in the linear viscoelastic regime at deformations low enough that the network properties, such as mesh size or connectivity, are unaffected by the applied shear. Experiments on vimentin, desmin and K8/K18 show that predominantly elastic networks with  $G' > G''$  are formed within seconds after starting the assembly [39,68]. The elasticity increases over time and it takes between 30 and 60 min to form mature networks with approximately time independent elastic properties. Typically,  $G'$  is a factor of 5 to 10 higher than  $G''$  for IF networks irrespective of the concentration of divalent ions [64,68]. Both quantities are nearly independent of frequency in the range between 0.01 and 10 rad/s [64,41,68,71–74] and  $G'$  is also termed plateau modulus  $G_0$ . This behavior is typical for gels and Yamada et al. could show for K8/K18 that  $G_0$  does not depend on filament length [73]. The linear viscoelastic properties of wild type proteins, mutations and tailless variants of the proteins at physiological pH are similar [37,75–77].

In general, entangled polymers without cross-links show gel- or rubber-like properties at intermediate frequencies but exhibit a transition to a terminal flow regime with  $G'' > G'$  and characteristic scaling laws  $G'' \sim \omega$  and  $G' \sim \omega^2$ . The frequency  $\omega_r$  at which  $G'' = G'$  characterizes this transition and the corresponding timescale  $\tau_r \sim \omega_r^{-1}$  is termed the longest relaxation time. This relaxation time increases or the respective

frequency decreases with increasing contour length of the polymer. Among the studied IF networks, K5/K14 is the only one for which such a characteristic relaxation time has been found [76]. The fast network formation of IFs, the absence of a finite relaxation time and the length independency of  $G_0$  indicate that even short filaments form cross-linked polymer networks. The plateau regime at intermediate frequencies with  $G' > G''$  is determined by the filament network. The linear viscoelastic properties in the high frequency regime are dominated by the stress relaxation of individual filaments. Accordingly, the plateau modulus  $G_0$  is related to the crosslink density and the high frequency moduli have been used to determine the persistence length of IFs as described above. The frequency dependency of  $G'$  and  $G''$  of a representative IF network is shown in Fig. 5A.

The mesh size  $\xi$  characterizes the average distance between adjacent cross-links. This important structural feature of IF networks can be directly determined by tracking the thermal motion of non-interacting tracer particles with different sizes [37,65]. Particles with diameter  $d < \xi$  can diffuse freely within the sample but if the filament network confines the particle motion the slope of the mean squared displacement (MSD) approaches zero (Fig. 5B). Vimentin forms networks consisting of single filaments even in the presence of 160 mM NaCl and 4 mM Mg<sup>2+</sup> [75]. Particle tracking experiments reveal that the mesh size of vimentin networks decreases upon addition of MgCl<sub>2</sub>

[65] (see Fig. 5B). K8/K18 assembles already in 10 mM Tris-HCl (pH 7.4). The contour length of the filament strands between adjacent cross-links  $l_c$  decreases in the presence of 0.5 mM MgCl<sub>2</sub> [67], at even higher concentrations of MgCl<sub>2</sub> ( $> 1$  mM) extensive bundling is observed [66–68].

The mesh size of IF networks can be calculated simply from the protein concentration assuming a cubic network constituted of rigid rods with corresponding mass per length  $\lambda$  [37,65]. Particle tracking experiments show that this geometric model recovers the mesh size reduction of vimentin networks upon addition of 2 mM MgCl<sub>2</sub>. For K8/K18 without divalent cations the mesh size is also well predicted. At a concentration of 1 g/l vimentin exhibits a mesh size between 1 and 2  $\mu\text{m}$  without divalent ions and between 0.5  $\mu\text{m}$  and 1  $\mu\text{m}$  when 2 mM MgCl<sub>2</sub> is added (Fig. 5B) [65]. For K8/K18 at the same concentration mesh size values between 0.2 and 0.5  $\mu\text{m}$  are reported [37]. The increase in mesh size of K8/K18 at 0.5 g/l expected under bundling conditions is not large enough that 1  $\mu\text{m}$  particles could diffuse through the mesh [67,68].

The magnitude and the scaling of the plateau modulus  $G_0$  with protein concentration of mature IF networks is directly related to  $l_c$ ,  $\xi$  and the thermal energy of the filaments [79–81]. The classical theory of rubber elasticity considers only the contribution of cross-links or entanglements to the free energy density and assumes that the polymers are in thermal equilibrium [79]. Each of these constraints reduces

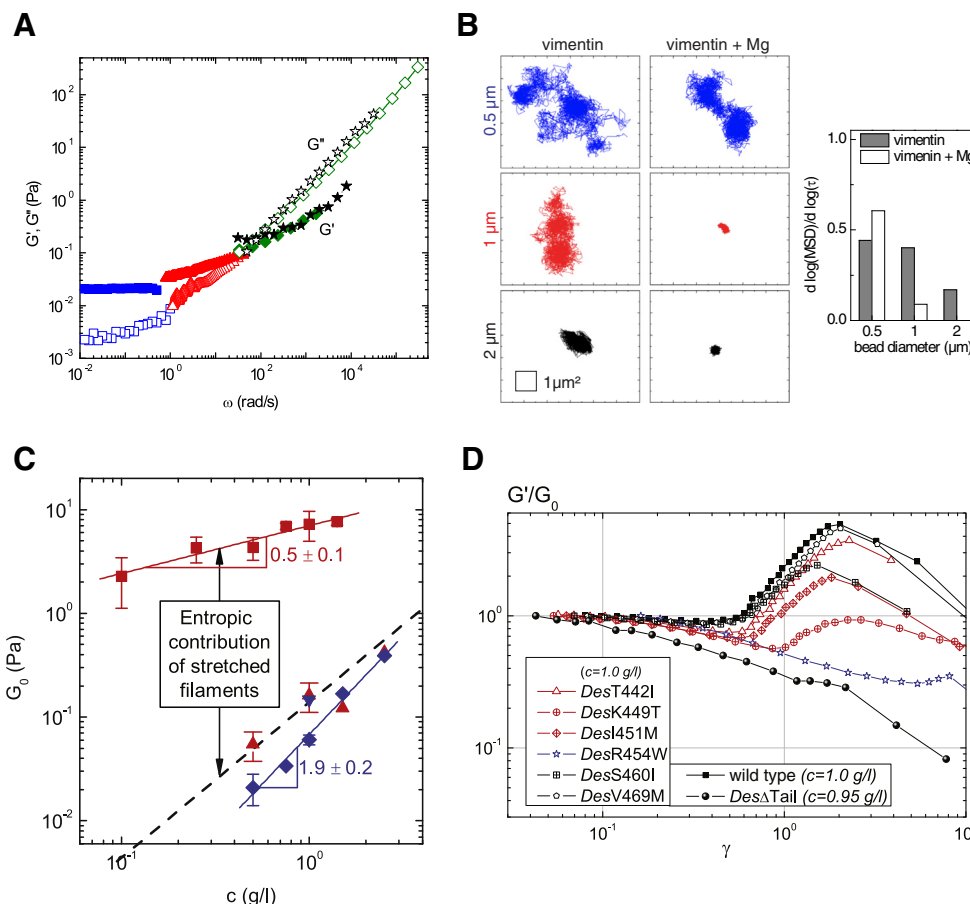


**Fig. 5.** (A) Frequency dependence of the linear viscoelastic moduli  $G'$  (closed symbols) and  $G''$  (open symbols) of K8/K18 (0.5 g/l) as obtained from shear rheology (squares), multiple particle tracking (red triangles), diffusing wave spectroscopy (green diamonds) and high frequency oscillatory squeeze flow (black stars); adapted from [36]. (B) Individual y-x tracks for microspheres with diameters of 0.5  $\mu\text{m}$  (top, blue), 1  $\mu\text{m}$  (center, red), 2  $\mu\text{m}$  (bottom, black) in vimentin (1 g/l, left column) and vimentin with 2 mM Mg<sup>2+</sup> (right column) and slope of the MSD at  $\tau = 10$  s; adapted from [64]. (C)  $G_0$  data obtained from shear rheology (red squares) and particle tracking (red triangles) as a function of K8/K18 concentration. The blue diamonds and the blue upside down triangles represent the values measured with Triton X-100 using bulk shear rheometry or particle tracking, respectively. The dotted line shows the results obtained from classical theory of rubber elasticity. Figure reprinted from [36]. (D) The reduced storage modulus  $G'/G_0$  of DesT442I, DesK449T, DesI451M, DesR454W, DesS460I, and DesV469M, as well as wild-type desmin and Des $\Delta$ Tail networks, as a function of strain amplitude. Except DesR454W, all mutations form apparently healthy filaments, in agreement with electron microscopy images revealing that these filaments are considerably shorter than wild-type desmin or the other mutants; figure reprinted from [76] Copyright 2009, with permission from Elsevier.

the degree of freedom of the system and increases the free energy by  $k_B T$ . This results in a plateau modulus of  $G_0 = k_B T / \xi^3$  because the density of topological constraints  $v$  is directly related to the mesh size  $\xi^{-3} = v$ . The *tube model* for entangled solutions of semi-flexible filaments includes the entanglement length  $l_e$  and describes the elasticity as  $G_0 \sim k_B T \xi^{-2} l_e^{-1}$  with  $l_e \sim \xi^{4/5} L_p^{1/5}$  [82], which results in scaling of  $G_0 \sim k_B T \xi^{-14/5} L_p^{-1/5}$  [78]. The *affine model* derives the elasticity from the thermal fluctuations of the filaments between cross-links or entanglements [80]. These fluctuations depend on the contour length between cross-links and the persistence length. The corresponding scaling law is  $G_0 \sim k_B T L_p^2 \xi^{-2} l_c^{-3}$ . Mesh size and contour length between entanglements or cross-links are similar if  $\xi \lesssim L_p$ . Assuming a cubic grid of filaments results in the following scaling of mesh size with protein concentration:  $\xi \sim c^{-0.5}$  [37,78,80]. According to classical theory of rubber elasticity the plateau modulus then scales with concentration as  $G_0 \sim c^{1.5}$  [37]. The tube model for semi-flexible filaments results in a scaling of  $G_0 \sim c^{1.4}$  [78]. The affine model predicts a scaling of  $G_0 \sim c^{2.25}$  [80,83].

Vimentin networks above concentrations of 1.5 g/l as well as neurofilaments without divalent cations exhibit scaling exponents of 1.3 [72,75] close to what is expected from rubber elasticity theory or the tube model for semi-flexible filaments. The scaling exponents found for vimentin [39,71,84], desmin [39] and keratin [68,73,84] networks at concentrations below 1.5 g/l exhibit scaling exponents between 0.3 and 0.7, which are much lower than the theoretical predictions and the mesh sizes calculated from  $G_0$  are much lower than obtained from particle tracking experiments [37]. This deviation is attributed to an entropically unfavorable stretched filament conformation between adjacent cross-links at low concentrations [37]. The attractions between filaments at their contact points needed to maintain such stretched configurations are provided by hydrophobic amino acid clusters located in the central rod domain [37]. Attraction of filaments is reduced and the strands can equilibrate when a non-ionic surfactant is added. In that case, the modulus values obtained from mechanical rheometry and particle tracking experiments agree very well and  $G_0$  scales with concentration as predicted by classical rubber elasticity theory (Fig. 5C, [37]). The properties of IF networks at higher protein concentrations and in the presence of  $MgCl_2$  follow the predictions by the affine model [41]. Surprisingly, most structural changes of IF networks due to mutations [76] or bundling [67,68] have no significant influence on their linear viscoelastic properties.

One of the most prominent mechanical features of cross-linked IF networks is their so-called "strain stiffening" behavior [37,39,41,68,71–77,84], this behavior is not unique to IFs, as other cross-linked biopolymer networks exhibit substantial strain stiffening as well. The apparent modulus of networks consisting of healthy IF proteins increases at large strains or stresses until the network ruptures at a critical deformation. The entropic nature of the elastic response to deformation and the strong attraction between IFs at their contact points give rise to this distinct behavior.

The affine model predicts that the critical strain  $\gamma_c$  at which the networks starts to stiffen depends linearly on  $l_c$  [80]. This approach has been used to determine the scaling of  $l_c$  with protein concentration  $c_{IF}$  and divalent salt ( $Mg^{2+}$ ) concentration  $c_{Mg}$ . For neurofilaments and vimentin  $l_c \sim c_{IF}^{-0.4}$  and  $l_c \sim c_{Mg}^{-0.2}$ , respectively, have been found [41]. The concentration dependence follows the scaling predicted by the cubic model assuming  $l_c \approx \xi$ . The critical strain of K8/K18 is concentration independent, which can be rationalized assuming that the filaments are more stretched at lower concentrations [68].

Networks can exhibit strain stiffening either if the filaments are permanently cross-linked [83] or if the system is trapped in a glassy state [85]. Within the framework of the so-called glassy wormlike chain model, the strength of reversible cross-links is characterized by the parameter  $\varepsilon$  and  $\varepsilon \rightarrow \infty$  corresponds to permanent crosslinking. Some studies show that vimentin and neurofilament networks behave

like permanently cross-linked gels [41,75]. Other studies of the nonlinear response [37,68,72] including creep experiments [71] suggest that IF networks exhibit reversibly breakable cross-links with a finite bond energy. Divalent cations do not change this characteristic feature but the stress at which the network ruptures increases [68,75]. The corresponding increase of the maximum elasticity is more pronounced than the increase  $G_0$  due to divalent cations, which can be rationalized by changes of the bond strength or changes of filament compliance in axial direction [86]. The protein sequence motif providing the strong attractions needed for strain stiffening is located in the tail domain. No strain stiffening is observed for proteins without tail domain. This has been verified for desmin [77], vimentin [75] and K8/K18 filaments [37]. Studies on mutations in the carboxy tail domain of desmin, which are involved in severe skeletal and cardiac myopathies, show that strain stiffening is of high physiological relevance. All these mutations form apparently healthy filaments and networks in cells and *in vitro* but exhibit a reduced strain stiffening (Fig. 5D, [77]). EBS (epidermolysis bullosa simplex) causing mutations of K5/K14 reduce the ability to crosslink at pH 7.0 and change the response from stiffening to softening [76]. Table 3 comprises the structural and rheological features and the influence of  $MgCl_2$  on representative networks of vimentin and K8/K18.

## 7. IFs and the physical properties of cells

The variability of IF primary structure between organisms and cell types and thus differing mechanical properties and charge interactions, as reviewed above, lead to the hypothesis that they are an important determinant of cell mechanics. Very timely and consistently with this idea, several studies on the influence of IFs on cell mechanics on a whole cell level have been performed. It is a great challenge to design the experiments in a way that an objective comparison to control cells is possible. Recently, with the availability of new cell lines [88], such experiments became possible and mechanical testing on whole cells has been performed using optical stretching forces [89] and AFM [90]. Consistently, in both works it was found that keratin contributes majorly to the mechanical stiffness in keratinocytes. The noncontact measurements using an optical stretcher reveal an increase in deformability by 60% for the keratin knockout cells compared to wild-type cells, which is much more than can be caused by depolymerizing actin in the cells [89]. AFM allows for direct measurement of the Young's modulus and the authors of Ref. [90] find a decrease from 752 Pa to 412 Pa from wild-type cells to keratin knockout cells for the cell body.

For vimentin IFs in whole cells, active microrheology involving optical tweezers showed, that they contribute little to cortical stiffness, but regulate intracellular mechanics [91]. Additionally, vimentin has been shown not to contribute to the force spectrum of the cellular interior [92]. Mendez et al. found that the microinjection of purified vimentin into MCF-7 cells leads to the formation of vimentin filaments and the

**Table 3**  
Structural and rheological properties of vimentin and K8/K18 networks.

	Vimentin	K8/K18
Mesh size $\xi \approx (3\lambda/c)^{0.5}$	$\lambda = 6.31 \cdot 10^{-11} \text{ g/m}$ [87]	$\lambda = 3.16 \cdot 10^{-11} \text{ g/m}$ [87]
Effect of $MgCl_2$	Increases cross-linking [64,74]	$\leq 1 \text{ mM}$ increases cross-linking $> 1 \text{ mM}$ bundling [67,68]
Elastic modulus	Weak concentration dependency at low concentrations [39,68,71,73,84] due to entropic contributions of stretched filaments [36,67]	Expected elastic properties at higher concentrations [75] or upon addition of surfactants [37,73]
Strain stiffening	Strain stiffening due to attractive interactions located in the tail domain [37,75]	Maximum elasticity before rupture increases upon addition of $MgCl_2$ [68,75]

epithelial cells acquire an elongated cell shape that mimics the one of mesenchymal cells. Most likely due to degradation of the vimentin this process is reversed over time [93]. Thus, cells can be “triggered” to adapt their properties by introducing IF proteins. The importance of the composite nature of the cytoskeletal network [1] has been highlighted by Gregor et al., who suggested that vimentin provides physical constraints to the acto-myosin system tightly connected to focal adhesions [94].

Both *in vitro* experiments on purified, reconstituted systems and whole cell experiments are important to tackle the role of IFs in cell mechanics from both sides, bottom-up and top-down. Simplified *in vitro* systems help to pin down principle mechanisms whereas the whole complexity of a living cell is difficult, probably impossible, to grasp from a physics standpoint, but the whole, living cell is ultimately our system of interest. As an example, the ionic strengths used in *in vitro* experiments (see Sections 3 and 4) are mostly much higher than the average concentrations found in cells. However, *locally* such high concentrations may well be found in living cells and ions, along with IF associated proteins (IFAPs) may contribute considerably to IF assembly, filament bundling, network formation and mechanical properties such as persistence length. IF networks in cells may even serve as an “ion buffer” due to their polyelectrolytic properties.

Additionally, few experiments investigating the properties of keratin bundle structures in their physiological context inside cells have been performed. Even though there are no known motors which interact directly with IFs, these keratin bundles are highly dynamic in cells. This dynamic nature applies to the formation and maturation of the bundles [95] as well as to the mature network of bundles. This motion can be suppressed by blebbistatin treatment of the cells [96] and thus might be due to acto-myosin activity and interlinking of actin and IF structures in cells. The bundle motion also decreases when the cells are exposed to external stresses, e.g., by microfluidic flow [96] and we interpreted this increase of persistence in the motion to be a consequence of  $\text{Ca}^{2+}$  influx via mechanosensitive ion channels, which in turn amplifies acto-myosin activity, thereby “stretching” the IF network and leading to less pronounced motion.

Looking at the individual bundles, which consist of several filaments, “buckling events” [97] are observed and from analyzing these buckling events, it was found that the individual filaments are quite strongly mechanically coupled within the bundle, but less coupled for thicker bundles [98]. This variability in coupling strength between the individual building blocks of the cellular structures may again be a way for cells to *locally* adapt their mechanical properties to functional requirements.

Apart from visible light microscopy, which offers the possibility to image living cells and fluorescently label molecules specifically, and EM, which reaches high spatial resolution, yet only in static samples, X-ray imaging as a third, complementary, method to image cells has been used to investigate keratin bundles. X-rays have the advantage that they penetrate matter easily and deeply and due to their short wavelengths they offer nm-resolution. Scanning nano-diffraction was used to image individual keratin bundles in cells and thereby combining information from real and from reciprocal space and local orientation and bundle structure could be resolved [99].

## 8. Conclusions

IFs are a prime example of a biological structure, where architecture and mechanical function are intrinsically linked: this aspect becomes most apparent in the enormous extensibility of IFs and their increased network elasticity at large stresses or deformations (strain-stiffening), but also in the weak concentration dependence of the equilibrium modulus. In recent years, applying physical methods to biological systems has led to much advance in the IF field. The impressive amount of biological and biochemical knowledge on that had already been collected for decades before, is now being complemented by studies on specifically the physical properties of these intriguing biological filaments and

their higher-order structures. The advent of state of the art experimental methods in the field of high resolution imaging, (automated) data analysis, and sophisticated mechanical testing has enabled these experiments along with simulation and modeling approaches.

It has already become clear that small changes in the amino acid sequence, e.g. between different IF types or between mutants, despite identical secondary structure, lead to large variations in the emerging filaments. The puzzle of similarities and differences between different types of IFs in their mechanical behavior and interaction properties still remains to be fully solved. Currently, researchers are working on bridging the gap between results from experiments on *in vitro* model systems and cell studies and an extension to the tissue level will be the next logical step. Ideally, biophysical research will thereby help solving biomedical questions.

## Conflict of interest

The authors declare no conflict of interest.

## Acknowledgements

The authors thank Harald Herrmann, Christian Dammann, Bernd Nöding, Jens Nolting, Britta Weinhausen, Martha Brennich and Clément Hémonnot for fruitful discussions and in particular Harald Herrmann for critically reading the manuscript. The work was financially supported by the Deutsche Forschungsgemeinschaft (DFG) in the framework of SFB 755 (B7, C10), project KO-3752/5-1, and the Cluster of Excellence and DFG Research Center Nanoscale Microscopy and Molecular Physiology of the Brain.

## References

- [1] F. Huber, A. Boire, M.P. López, G.H. Koenderink, Cytoskeletal crosstalk: when three different personalities team up, *Curr. Opin. Struct. Biol.* 32C (2015) 39–47.
- [2] A. Robert, H. Herrmann, M.W. Davidson, V.I. Gelfand, Microtubule-dependent transport of vimentin filament precursors is regulated by actin and by the concerted action of Rho- and p21-activated kinases, *FASEB J.* 28 (2014) 2879–2890.
- [3] C. Hookway, L. Ding, M.W. Davidson, J.Z. Rapoport, G. Danuser, V.I. Gelfand, Microtubule-dependent transport and dynamics of vimentin intermediate filaments, *Mol. Biol. Cell* 26 (2015) 1675–1686 <http://www.molbiocell.org/content/26/9/1675>.
- [4] K.J. Green, M. Bohringer, T. Gocken, J.C. Jones, Intermediate filament associated proteins, *Adv. Protein Chem.* 70 (2005) 143–202.
- [5] M.J. Castanon, G. Walko, L. Winter, G. Wiche, Plectin-intermediate filament partnership in skin, skeletal muscle, and peripheral nerve, *Histochem. Cell Biol.* 140 (2013) 33–53.
- [6] H. Herrmann, M. Häner, M. Brettel, S.A. Müller, K.N. Goldie, B. Fedtke, A. Lustig, W.W. Franke, U. Aebi, Structure and assembly properties of the intermediate filament protein vimentin: the role of its head, rod and tail domains, *J. Mol. Biol.* 264 (1996) 933–953.
- [7] R. Kirmse, S. Portet, N. Mücke, U. Aebi, H. Herrmann, J. Langowski, A quantitative kinetic model for the *in vitro* assembly of intermediate filaments from tetrameric vimentin, *J. Mol. Biol.* 282 (2007) 18563–18572.
- [8] H. Herrmann, M. Häner, M. Brettel, N.-O. Ku, U. Aebi, Characterization of distinct early assembly units of different intermediate filament proteins, *J. Mol. Biol.* 286 (1999) 1403–1420.
- [9] T. Lichtenstern, N. Mücke, U. Aebi, M. Mauermann, H. Herrmann, Complex formation and kinetics of filament assembly exhibited by the simple epithelial keratins K8 and K18, *J. Struct. Biol.* 177 (2012) 54–62.
- [10] S. Portet, N. Mücke, R. Kirmse, J. Langowski, M. Beil, H. Herrmann, Vimentin intermediate filament formation: *in vitro* measurement and mathematical modeling of the filament length distribution during assembly, *Langmuir* 25 (2009) 8817–8823.
- [11] A.V. Sokolova, L. Kreplak, T. Wedig, N. Mücke, D.I. Svergun, H. Herrmann, U. Aebi, S.V. Strelkov, Monitoring intermediate filament assembly by small-angle X-ray scattering reveals the molecular architecture of assembly intermediates, *Proc. Natl. Acad. Sci. U. S. A.* 103 (2006) 16206–16211.
- [12] M.E. Brennich, S. Bauch, U. Vainio, T. Wedig, H. Herrmann, S. Köster, Impact of ion valency on the assembly of vimentin studied by quantitative small angle X-ray scattering, *Soft Matter* 10 (2014) 2059–2068.
- [13] M.E. Brennich, J.-F. Nolting, C. Dammann, B. Nöding, S. Bauch, H. Herrmann, T. Pfohl, S. Köster, Dynamics of intermediate filament assembly followed in micro-flow by small angle X-ray scattering, *Lab Chip* 11 (2011) 708–716.
- [14] A.C. Steven, J.F. Hainfeld, B.L. Trus, J.S. Wall, P.M. Steinert, The distribution of mass in heteropolymer intermediate filaments assembled *in vitro*. Stem analysis of vimentin/desmin and bovine epidermal keratin, *J. Biol. Chem.* 258 (1983) 8323–8329.

- [15] A. Engel, R. Eichner, U. Aebi, Polymorphism of reconstituted human epidermal keratin filaments: determination of their mass-per-length and width by scanning transmission electron microscopy (STEM), *J. Ultrastruct. Res.* 90 (1985) 323–335.
- [16] T. Mitchison, M. Kirschner, Dynamic instability of microtubule growth, *Nature* 312 (1984) 237–242.
- [17] J.R. Kuhn, T.D. Pollard, Real-time measurements of actin filament polymerization by total internal reflection fluorescence microscopy, *Biochem. J.* 388 (2005) 1387–1402.
- [18] G. Çolakoglu, A. Brown, Intermediate filaments exchange subunits along their length and elongate by end-to-end annealing, *J. Cell Biol.* 185 (2009) 769–777.
- [19] A. Uchida, G. Colakoglu, L. Wang, P.C. Monsma, A. Brown, Severing and end-to-end annealing of neurofilaments in neurons, *Proc. Natl. Acad. Sci. U. S. A.* 110 (2013) E2696–E2705.
- [20] S. Winheim, A.R. Hieb, M. Silbermann, E.-M. Surmann, T. Wedig, H. Herrmann, J. Langowski, N. Mücke, Deconstructing the late phase of vimentin assembly by total internal reflection fluorescence microscopy (TIRFM), *PLoS One* 6 (2011) e19202.
- [21] B. Nöding, H. Herrmann, S. Köster, Direct observation of subunit exchange along mature vimentin intermediate filaments, *Biochem. J.* 107 (2014) 2923–2931.
- [22] K.L. Vikstrom, G.G. Borisy, R.D. Goldman, Dynamic aspects of intermediate filament networks in BHK-21 cells, *Proc. Natl. Acad. Sci. U. S. A.* 86 (1989) 549–553.
- [23] J. Ngai, T.R. Coleman, E. Lazarides, Localization of newly synthesized vimentin subunits reveals a novel mechanism of intermediate filament assembly, *Cell* 60 (1990) 415–427.
- [24] T.R. Coleman, E. Lazarides, Continuous growth of vimentin filaments in mouse fibroblasts, *J. Cell Sci.* 103 (1992) 689–698.
- [25] P. Soellner, R.A. Quinlan, W.W. Franke, Identification of a distinct soluble subunit of an intermediate filament protein: tetrameric vimentin from living cells, *Proc. Natl. Acad. Sci. U. S. A.* 82 (1985) 7929–7933.
- [26] K.L. Vikstrom, S.S. Lim, R.D. Goldman, C.G. Borisy, Steady state dynamics of intermediate filament networks, *J. Cell Biol.* 118 (1992) 121–129.
- [27] Y.-H. Chou, S. Khoun, H. Herrmann, R.D. Goldman, Nestin promotes the phosphorylation-dependent disassembly of vimentin intermediate filaments during mitosis, *Mol. Biol. Cell* 14 (2003) 1468–1478.
- [28] J.E. Eriksson, T. He, A.V. Trejo-Skalli, A.-S. Härmälä-Braskén, J. Hellman, Y.-H. Chou, R.D. Goldman, Specific *in vivo* phosphorylation sites determine the assembly dynamics of vimentin intermediate filaments, *J. Cell Sci.* 117 (2004) 919–932.
- [29] M. Hesse, T.M. Magin, K. Weber, Genes for intermediate filament proteins and the draft sequence of the human genome: novel keratin genes and a surprisingly high number of pseudogenes related to keratin genes 8 and 18, *J. Cell Sci.* 114 (2001) 2569–2575.
- [30] M.B. Omary, P.A. Coulombe, W.H. Irwin McLean, Intermediate filament proteins and their associated diseases, *N. Engl. J. Med.* 351 (2004) 2087–2100.
- [31] M.B. Omary, “IF-pathies”: a broad spectrum of intermediate filament-associated diseases, *J. Clin. Invest.* 119 (2009) 1756–1762.
- [32] H. Herrmann, S.V. Strelkov, History and phylogeny of intermediate filaments: now in insects, *BMC Biol.* 9 (2011) 16.
- [33] F. Gittes, B. Mickey, J. Nettleton, J. Howard, Flexural rigidity of microtubules and actin filaments measured from thermal fluctuations in shape, *J. Cell Biol.* 120 (1993) 923–934.
- [34] B. Nöding, S. Köster, Intermediate filaments in small configuration spaces, *Phys. Rev. Lett.* 108 (2012) 088101.
- [35] S. Köster, D.A. Weitz, R.D. Goldman, U. Aebi, H. Herrmann, Intermediate filament mechanics in vitro and in the cell: from coiled coils to filaments, fibers and networks, *Curr. Opin. Struct. Biol.* 32C (2015) 82–91.
- [36] D.S. Fudge, K.H. Gardner, V.T. Forsyth, C. Riekel, J.M. Gosline, The mechanical properties of hydrated intermediate filaments: insights from hagfish slime threads, *Biochem. J.* 385 (2003) 2015–2027.
- [37] P. Pawelzyk, N. Mücke, H. Herrmann, N. Willenbacher, Attractive interactions among intermediate filaments determine network mechanics in vitro, *PLoS One* 9 (2014) e93194.
- [38] M. Hohenadl, T. Storz, H. Kirpal, K. Kroy, R. Merkel, Desmin filaments studied by quasi-elastic light scattering, *Biochem. J.* 77 (1999) 2199–2209.
- [39] M. Schopferer, H. Bär, B. Hochstein, S. Sharma, N. Mücke, H. Herrmann, N. Willenbacher, Desmin and vimentin intermediate filament networks: their viscoelastic properties investigated by mechanical rheometry, *J. Mol. Biol.* 388 (2009) 133–143.
- [40] N. Mücke, L. Kreplak, R. Kirmse, T. Wedig, H. Herrmann, U. Aebi, J. Langowski, Assessing the flexibility of intermediate filaments by atomic force microscopy, *J. Mol. Biol.* 335 (2004) 1241–1250.
- [41] Y.-C. Lin, N.Y. Yao, C.P. Broedersz, H. Herrmann, F.C. MacKintosh, D.A. Weitz, Origins of elasticity in intermediate filament networks, *Phys. Rev. Lett.* 104 (2010) 058101.
- [42] R. Beck, J. Deek, M.C. Choi, T. Ikawa, O. Watanabe, E. Frey, P. Pincus, C.R. Safinya, Unconventional salt trend from soft to stiff in single neurofilament biopolymers, *Langmuir* 26 (2010) 18595–18599.
- [43] Z. Dogic, J. Zhang, A.W.C. Lau, H. Aranda-Espinoza, P. Dalheimer, D.E. Discher, P.A. Janmey, R.D. Kamien, T.C. Lubensky, A.G. Yodh, Elongation and fluctuations of semiflexible polymers in a nematic solvent, *Phys. Rev. Lett.* 92 (2004) 125503.
- [44] F. Gittes, F. MacKintosh, Dynamic shear modulus of a semiflexible polymer network, *Phys. Rev. E* 58 (1998) R1241.
- [45] K.N. Goldie, T. Wedig, A.K. Mitra, U. Aebi, H. Herrmann, A. Hoenger, Dissecting the 3-D structure of vimentin intermediate filaments by cryo-electron tomography, *J. Struct. Biol.* 158 (2007) 378–385.
- [46] L. Kreplak, H. Bär, J.F. Leterrier, H. Herrmann, U. Aebi, Exploring the mechanical behavior of single intermediate filaments, *J. Mol. Biol.* 354 (2005) 569–577.
- [47] L. Kreplak, H. Herrmann, U. Aebi, Tensile properties of single desmin intermediate filaments, *Biochem. J.* 94 (2008) 2790–2799.
- [48] C. Guzmán, S. Jeney, L. Kreplak, S. Kasas, A.J. Kulik, U. Aebi, L. Forró, Exploring the mechanical properties of single vimentin intermediate filaments by atomic force microscopy, *J. Mol. Biol.* 360 (2006) 623–630.
- [49] B. Ramm, J. Stigler, M. Hinczewski, D. Thirumalai, H. Herrmann, G. Woehlke, M. Rief, Sequence-resolved free energy profiles of stress-bearing vimentin intermediate filaments, *Proc. Natl. Acad. Sci. U. S. A.* 111 (2014) 11359–11364.
- [50] E.G. Bendit, A quantitative X-ray diffraction study of the alpha–beta transformation in wool keratin, *Text. Res. J.* 30 (1960) 547–555.
- [51] L. Kreplak, D. Fudge, Biomechanical properties of intermediate filaments: from tissues to single filaments and back, *Bioessays* 29 (2007) 26–35.
- [52] Z. Qin, L. Kreplak, M.J. Buehler, Hierarchical structure controls nanomechanical properties of vimentin intermediate filaments, *PLoS One* 4 (2009) e7294.
- [53] Z. Qin, L. Kreplak, M.J. Buehler, Nanomechanical properties of vimentin intermediate filament dimers, *Nanotechnology* 20 (2009) 425101.
- [54] Z. Qin, M.J. Buehler, Structure and dynamics of human vimentin intermediate filament dimer and tetramer in explicit and implicit solvent models, *J. Mol. Model.* 17 (2011) 37–48.
- [55] C. Dammann, H. Herrmann, S. Köster, Competitive counterion binding regulates the aggregation onset of vimentin intermediate filaments, *Isr. J. Chem.* (2015), <http://dx.doi.org/10.1002/ijch.201400153>.
- [56] P.A. Janmey, D.R. Slochower, Y.-H. Wang, Q. Wen, A. Cebers, Polyelectrolyte properties of filamentous biopolymers and their consequences in biological fluids, *Soft Matter* 10 (2014) 1439–1449.
- [57] J. Kayser, H. Grabmayr, M. Harasim, H. Herrmann, A.R. Bausch, Assembly kinetics determine the structure of keratin networks, *Soft Matter* 8 (2012) 8873–8879.
- [58] C. Dammann, B. Nöding, S. Köster, Vimentin networks at tunable ion-concentration in microfluidic drops, *Biomicrofluidics* 6 (2012) 22009–2200910.
- [59] H. Herrmann, U. Aebi, Intermediate filament assembly: fibrilllogenesis is driven by decisive dimer–dimer interactions, *Curr. Opin. Struct. Biol.* 8 (1998) 177–185.
- [60] M.H. Stromer, M.A. Ritter, Y.Y. Pang, R.M. Robson, Effect of cations and temperature on kinetics of desmin assembly, *Biochem. J.* 246 (1987) 75–81.
- [61] I. Hofmann, H. Herrmann, W.W. Franke, Assembly and structure of calcium-induced thick vimentin filaments, *Eur. J. Cell Biol.* 56 (1991) 328–341.
- [62] M. Kooijman, M. Bloemendal, P. Traub, R. van Grondelle, H. van Amerongen, Transient electric birefringence study of intermediate filament formation from vimentin and glial fibrillary acidic protein, *J. Biol. Chem.* 272 (1997) 22548–22555.
- [63] M. Kooijman, M. Bloemendal, P. Traub, R. van Grondelle, H. van Amerongen, Hydrodynamic and electrical characterization of T-vimentin dimers and tetramers by transient electric birefringence measurements, *J. Biol. Chem.* 270 (1995) 2931–2937.
- [64] Y.-C. Lin, C.P. Broedersz, A.C. Rowat, T. Wedig, H. Herrmann, F.C. MacKintosh, D.A. Weitz, Divalent cations crosslink vimentin intermediate filament tail domains to regulate network mechanics, *J. Mol. Biol.* 399 (2010) 637–644.
- [65] S. Köster, Y.-C. Lin, H. Herrmann, D.A. Weitz, Nanomechanics of vimentin intermediate filament networks, *Soft Matter* 6 (2010) 1910–1914.
- [66] J. Kayser, M. Haslbeck, L. Dempfle, M. Krause, C. Grashoff, J. Buchner, H. Herrmann, A.R. Bausch, The small heat shock protein Hsp27 affects assembly dynamics and structure of keratin intermediate filament networks, *Biochem. J.* 105 (2013) 1778–1785.
- [67] A. Leitner, T. Paust, O. Marti, P. Walther, H. Herrmann, M. Beil, Properties of intermediate filament networks assembled from keratin 8 and 18 in the presence of Mg<sup>2+</sup>, *Biochem. J.* 103 (2012) 195–201.
- [68] P. Pawelzyk, N. Willenbacher, H. Herrmann, Mechanics of intermediate filament networks assembled from keratins K8 and K18, *Soft Matter* 9 (2013) 8871–8880.
- [69] C. Dammann, S. Köster, Dynamics of counterion-induced attraction between vimentin filaments followed in microfluidic drops, *Lab Chip* 14 (2014) 2681–2687.
- [70] Q. Wen, P.A. Janmey, Polymer physics of the cytoskeleton, *Curr. Opin. Solid State Mater. Sci.* 15 (2011) 177–182.
- [71] P.A. Janmey, U. Euteneuer, P. Traub, M. Schliwa, Viscoelastic properties of vimentin compared with other filamentous biopolymer networks, *J. Cell Biol.* 113 (1991) 155–160.
- [72] S. Rammensee, P.A. Janmey, A.R. Bausch, Mechanical and structural properties of in vitro neurofilament hydrogels, *Eur. Biophys. J.* 36 (2007) 661–668.
- [73] S. Yamada, D. Wirtz, P.A. Coulombe, The mechanical properties of simple epithelial keratins 8 and 18: discriminating between interfacial and bulk elasticities, *J. Struct. Biol.* 143 (2003) 45–55.
- [74] N.Y. Yao, C.P. Broedersz, Y.-C. Lin, K.E. Kasza, F.C. MacKintosh, D.A. Weitz, Elasticity in ionically cross-linked neurofilament networks, *Biochem. J.* 98 (2010) 2147–2153.
- [75] Y.-C. Lin, C.P. Broedersz, A.C. Rowat, T. Wedig, H. Herrmann, F.C. MacKintosh, D.A. Weitz, Divalent cations crosslink vimentin intermediate filament tail domains to regulate network mechanics, *J. Mol. Biol.* 399 (2010) 637–644.
- [76] L. Ma, S. Yamada, D. Wirtz, P.A. Coulombe, A ‘hot-spot’ mutation alters the mechanical properties of keratin filament networks, *Nat. Cell Biol.* 3 (2001) 503–506.
- [77] H. Bär, M. Schopferer, S. Sharma, B. Hochstein, N. Mücke, H. Herrmann, N. Willenbacher, Mutations in desmin’s carboxy-terminal “tail” domain severely modify filament and network mechanics, *J. Mol. Biol.* 397 (2010) 1188–1198.
- [78] B. Hinner, M. Tempel, E. Sackmann, K. Kroy, E. Frey, Entanglement, elasticity, and viscous relaxation of actin solutions, *Phys. Rev. Lett.* 81 (1998) 2614–2617.
- [79] P.-G. de Gennes, *Scaling Concepts in Polymer Physics*, Cornell Univ., Pr, Ithaca, 1979.
- [80] F.C. MacKintosh, J. Käs, P.A. Janmey, Elasticity of semiflexible biopolymer networks, *Phys. Rev. Lett.* 75 (1995) 4425–4428.
- [81] S.P. Obukhov, M. Rubinstein, R.H. Colby, Network modulus and superelasticity, *Macromolecules* 27 (1994) 3191–3198.
- [82] H. Isambert, A.C. Maggs, Dynamics and rheology of actin solutions, *Macromolecules* 29 (1996) 1036–1040.
- [83] M.L. Gardel, J.H. Shin, F.C. MacKintosh, L. Mahadevan, P. Matsudaira, D.A. Weitz, Elastic behavior of cross-linked and bundled actin networks, *Science* 304 (2004) 1301–1305.

- [84] L. Ma, J. Xu, P.A. Coulombe, D. Wirtz, Keratin filament suspensions show unique micromechanical properties, *J. Biol. Chem.* 274 (1999) 19145–19151.
- [85] K. Kroy, J. Glaser, The glassy wormlike chain, *New J. Phys.* 9 (2007) 416.
- [86] C. Storm, J.J. Pastore, F.C. MacKintosh, T.C. Lubensky, P.A. Janmey, Nonlinear elasticity in biological gels, *Nature* 435 (2005) 191–194.
- [87] H. Herrmann, T. Wedig, R.M. Porter, E.B. Lane, U. Aebi, Characterization of early assembly intermediates of recombinant human keratins, *J. Struct. Biol.* 137 (2002) 82–96.
- [88] C. Kröger, F. Loschke, N. Schwarz, R. Windoffer, R.E. Leube, T.M. Magin, Keratins control intercellular adhesion involving PKC- $\alpha$ -mediated desmoplakin phosphorylation, *J. Cell Biol.* 201 (2013) 681–692.
- [89] K. Seltmann, A.W. Fritsch, J.A. Käs, T.M. Magin, Keratins significantly contribute to cell stiffness and impact invasive behavior, *Proc. Natl. Acad. Sci. U. S. A.* 110 (2013) 18507–18512.
- [90] L. Ramms, G. Fabris, R. Windoffer, N. Schwarz, R. Springer, C. Zhou, J. Lazar, S. Stiefel, N. Hersch, U. Schnakenberg, T.M. Magin, R.E. Leube, R. Merkel, B. Hoffmann, Keratins as the main component for the mechanical integrity of keratinocytes, *Proc. Natl. Acad. Sci. U. S. A.* 110 (2013) 18513–18518.
- [91] M. Guo, A.J. Ehrlicher, S. Mohammad, H. Fabich, M.H. Jensen, J.R. Moore, J.J. Fredberg, R.D. Goldman, D.A. Weitz, The role of vimentin intermediate filaments in cortical and cytoplasmic mechanics, *Biochem. J.* 105 (2013) 1562–1568.
- [92] M. Guo, A.J. Ehrlicher, M.H. Jensen, M. Renz, J.R. Moore, R.D. Goldman, J. Lippincott-Schwartz, F.C. MacKintosh, D.A. Weitz, Probing the stochastic, motor-driven properties of the cytoplasm using force spectrum microscopy, *Cell* 158 (2014) 822–832.
- [93] M.G. Mendez, S.-I. Kojima, R.D. Goldman, Vimentin induces changes in cell shape, motility, and adhesion during the epithelial to mesenchymal transition, *FASEB J.* 24 (2010) 1838–1851.
- [94] M. Gregor, S. Osmanagic-Myers, G. Burgstaller, M. Wolfram, I. Fischer, G. Walko, G.P. Resch, A. Jörgl, H. Herrmann, G. Wiche, Mechanosensing through focal adhesion-anchored intermediate filaments, *FASEB J.* 28 (2014) 715–729.
- [95] R. Windoffer, M. Beil, T.M. Magin, R.E. Leube, Cytoskeleton in motion: the dynamics of keratin intermediate filaments in epithelia, *J. Cell Biol.* 194 (2011) 669–678.
- [96] J.-F. Nolting, S. Köster, Influence of microfluidic shear on keratin networks in living cells, *New J. Phys.* 15 (2013) 045025.
- [97] C.P. Brangwynne, G.H. Koenderink, F.C. MacKintosh, D.A. Weitz, Nonequilibrium microtubule fluctuations in a model cytoskeleton, *Phys. Rev. Lett.* 100 (2008) 118104.
- [98] J.-F. Nolting, W. Möbius, S. Köster, Mechanics of individual keratin bundles in living cells, *Biochem. J.* 107 (2014) 2693–2699.
- [99] B. Weinhausen, J.-F. Nolting, C. Olenckowitz, J. Langfahl-Klabes, M. Reynolds, T. Salditt, S. Köster, X-ray nano-diffraction on cytoskeletal networks, *New J. Phys.* 14 (2012) 085013.